ELSEVIER

Cognitive Brain Research 15 (2002) 1–15

BRAIN RESEARCH INTERACTIVE

www.bres-interactive.com

Interactive report

The temporal dynamics of the effects in occipital cortex of visual-spatial selective attention

M.G. Woldorff[a,b,*], M. Liotti[c], M. Seabolt[d], L. Busse[a,b], J.L. Lancaster[d], P.T. Fox[d]

[a]*Center for Cognitive Neuroscience, Duke University, Box 90999, Durham, NC 27708-0999, USA*
[b]*Department of Psychological and Brain Sciences, Duke University, Durham, NC, USA*
[c]*Department of Psychology, University of Aberdeen, Aberdeen, Scotland, UK*
[d]*Research Imaging Center, UTHSCSA, San Antonio, TX, USA*

Accepted 8 September 2002

Abstract

The temporal dynamics of the effects of lateralized visual selective attention within the lower visual field were studied with the combined application of event-related potentials (ERPs) and positron emission tomography (^{15}O PET). Bilateral stimuli were rapidly presented to the lower visual field while subjects either passively viewed them or covertly attended to a designated side to detect occasional targets. Lateralized attention resulted in strongly enhanced PET activity in contralateral *dorsal* occipital cortex, while ERPs showed an enhanced positivity (P1 effect, 80–160 ms) for all stimuli (both non-targets and targets) over contralateral occipital scalp. Dipole modeling seeded by the dorsal occipital PET foci yielded an excellent fit for the peak P1 attention effect. However, more detailed ERP modeling throughout the P1 latency window (90–160 ms) suggested a spatial–temporal movement of the attention-related enhancement that roughly paralleled the shape of the dorsal occipital PET attention-related activations—likely reflecting the sequential attention-related enhancement of early visual cortical areas. Lateralized spatial attention also resulted in a longer-latency contralateral enhanced negativity (N2 effect, 230–280 ms) with a highly similar distribution to the earlier P1 effect. Dipole modeling seeded by the same dorsal occipital PET foci also yielded an excellent fit. This pattern of results provides evidence for re-entrance of attention-enhanced activation to the same retinotopically organized region of dorsal extrastriate cortex. Finally, target stimuli in the attended location elicited an additional prolonged enhancement of the longer-latency negativity over contralateral occipital cortex. The combination of PET activation and dipole modeling suggested contribution from a ventral-occipital generator to this target-related activity.

Theme: Neural basis of behavior

Topic: Cognition

Keywords: Attention; Dipole modeling; Multimodal imaging; Retinotopy; Re-entrant processing

1. Introduction

The functional brain imaging methodologies of positron emission tomography (PET) and functional magnetic resonance (fMRI) have contributed substantially to our understanding of which areas of the brain are involved in the processes underlying visual attention (reviewed in Refs. [5,34]). For example, several studies have indicated that attentional processing of a particular feature of a visual display (e.g. color, motion) enhances activity in the visual areas specialized for the processing of that feature [4,31]. Similarly, several studies have indicated that *sustained* visual spatial attention to a region of the visual field causes increased activity in the same low-level, retinotopically organized, visual areas that process information from that region of space [13,26,41,44].

Hemodynamically-based neuroimaging techniques (PET and fMRI) are powerful tools for mapping brain areas activated during various cognitive tasks. However, their temporal resolution is limited by the slow speed and the sluggishness of the hemodynamic response, which is of the order of seconds [1]. Therefore, the effects of attention in

*Corresponding author. Tel.: +1-919-681-0604; fax: +1-919-681-0815.
E-mail address: woldorff@duke.edu (M.G. Woldorff).

0926-6410/02/$ – see front matter
PII: S0926-6410(02)00212-4

various visual sensory-processing areas that have been observed with hemodynamic imaging provide little or no information about the timing or sequence of the enhanced activity in these areas.

Brain activity can be measured with high temporal resolution in vivo in humans by recording event-related electrical potentials (ERPs) from the scalp. Sustained attention to a region of space is reflected electrophysiologically by a modulation of several ERP components when attended stimuli are compared to unattended stimuli presented at that region. The earliest attentional enhancement in the visual ERP is the 'P1 effect', an increased early positivity over occipital cortex contralateral to the direction of attention (80–130 milliseconds) that is evoked by all stimuli presented to the attended location [12,14,15]. The early onset of the P1 attention effect (70 milliseconds) for all the attended-region stimuli, along with its contralateral occipital distribution, provided strong support for psychological theories of early selection (e.g. Ref. [17]), in that they provide compelling neurophysiological evidence that attention can influence relatively early sensory processing [14].

Although the temporal resolution of ERPs is extremely high (milliseconds), their spatial resolution is much coarser, and the determination of the sources of activity more difficult. Therefore, combining PET or fMRI measures (high spatial resolution) and ERP measures (high temporal resolution) of brain activity allows for both the precise localization of the neural regions that are affected by attention, as well as the timing and sequence of the attention-related modulations [6,7,9,24,35].

Despite the apparent complementarity of ERPs and hemodynamic techniques, relatively few studies have actually combined these very different measures of brain activity. A seminal study that employed ERPs and PET to investigate lateralized visual spatial attention to bilateral *upper visual field* stimuli was by Heinze et al. [13]. The authors found enhanced attention-related PET activations in the contralateral *ventral occipital* cortex and the early attention-enhanced ERP positivity over the contralateral occipital scalp (P1 effect). In addition, by seeding the ERP dipole-source modeling algorithm with the foci of the PET activity, the contralateral fusiform gyrus was shown to be the likely source for the P1 attention effect. This result provided strong evidence that focused visual spatial attention could modulate early sensory processing in low-level visual cortex. A second complementary combined PET/ERP study of lateralized visual spatial attention by Woldorff et al. [44] using bilateral stimuli in the *lower visual field* found strong attentional enhancements of PET activations in the *dorsal occipital* (DO) cortex contralateral to the direction of attention. Dipole source analysis of the ERP activity at the peak of the P1 attention effect placed its source in the same dorsal occipital region. Since the representation of the lower visual field is in the contralateral DO cortex, these results, in conjunction with those of Heinze et al. [13], provided strong evidence that the early, sustained, spatial attention effects follow the retinotopic organization of the visual sensory input pathways.

Other studies have further explored the issue of retinotopic organization of sustained visual attention effects. Mangun et al. [25], for example, found that increased load/difficulty in a sustained attention task (in which stimuli were presented to the upper visual field) enhanced the magnitude of both *ventral*-occipital lateralized hemodynamic (fMRI) attention effects and the corresponding ERP P1 attention effects. Recent developments in fMRI techniques have made it possible to create maps of the retinotopic organization of visual sensory areas and to delineate the different areas of early visual cortex. Overlaying functional spatial attention activations on these retinotopic maps of visual cortex, various studies [2,26,41] have now reported that attention to a particular region of space results in enhanced activation of those portions of the low-level visual areas that perform the primary sensory analyses of those particular regions of space. These results point towards a high degree of specificity to the retinotopic organization of the hemodynamic attention effects.

In the combined electrophysiological/hemodynamic studies of Woldorff et al. [44], as well as in the Mangun et al. [25] and Heinze et al. [13] studies, the main focus in the ERP/hemodynamic integration was on mapping *one* brain activation location (the centroid of the main occipital PET attention effect) to *one* point in time in the ERP epoch (the peak of the early P1 attention effect). Thus, there has as yet not been a delineation of the temporal *sequence* of attention-related activations in the various early visual areas in humans, nor any thorough analysis of the relationship between the longer-latency ERP attention effects and the hemodynamic occipital effects. One particularly important issue that can be explored with such a combined approach is whether the attentional effects are enhancements of early activity in the low-level sensory areas, or whether the attentional effects include late-selection re-entrant processes to these areas, or both.

Recurrent activation of low-level sensory regions has been postulated to play an important role in cognitive processes such as visual imagery, object recognition and attention. Large scale computer simulation models of the visual system, for example, have shown that re-entrant interactions between perceptual (posterior) areas and executive (anterior) areas could help accomplish visual feature integration (i.e. Refs. [21,40]). In addition, hemodynamic data in visual imagery (reviewed in Ref. [18]) and attention (see Ref. [38] for a meta-analysis of nine PET studies contrasting active visual discrimination to passive viewing) have provided a basis for a top-down modulation of activity in anatomically early visual areas. However, hemodynamic studies, by themselves, do not have the temporal resolution to determine the timing of any of the effects seen in low-level visual areas, and thus cannot indicate whether any such effects are re-entrant or not. Thus, neither the hemodynamic data nor the computer models provide any empirical information as to the

temporal dynamics of low-level attention effects (i.e. if early or late in processing).

The aim of the present paper was to delineate the spatio–temporal characteristics of the effects of covert visual spatial attention across the entire ERP epoch period, rather than just those at the peak of the P1, and to study the relationship of this activity across time to various portions of the spatially extensive PET activations in occipital cortex. We hypothesized that the ERP attention effects would reflect the spatial–temporal sequence of attention-related activity in the early, retinotopically organized visual areas. In addition, we expected that longer-latency ERP attention effects might, at least in part, reflect *re-entrant* activation of these same areas. Studying these relationships across time and neuroanatomy in this way were aimed at more fully elucidating the functional organization of visual spatial attention.

2. Methods

2.1. Subjects

Ten normal, healthy subjects participated in the experiment. They ranged in age from 18 to 41 years (mean 27 years) and were all right-handed. All subjects gave written informed consent for their participation.

2.2. Stimuli and task

In separate sessions, subjects performed the same visual attention tasks while either ERPs or PET scans of their brain activity were recorded. Subjects fixated on a small central cross while bilateral stimuli were flashed in the lower visual field at a rapid rate (interstimulus intervals (ISI)=250–750 ms). Each bilateral stimulus consisted of two small checkerboard arrays (one in each lower visual field quadrant), which alternated in black-and-white polarity in successive trials and which could have either one, two, or no small dots in them (Fig. 1). During different runs, subjects were instructed to attend to either the left or the right side of the bilateral arrays (‘attend-left’, ‘attend-right’), or to simply passively view the stimuli (‘passive’). In the active attention conditions, subjects attended covertly to the designated side and pressed a button with the right hand upon detecting the ‘target’ stimuli on that side (checkerboards with two dots). All stimuli with only one or no dots in the checkerboard array on the attended side were thus non-targets, or ‘standards’.

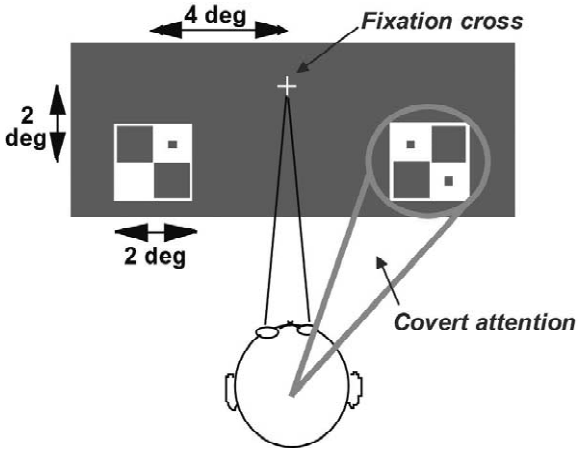

Fig. 1. Schematic diagram of the bilateral lower-field visual stimulus and an example of the visual spatial attention task for an attend-right condition.

Target frequency was either 2% or 16% in different runs, but the data were collapsed across target frequency in this report. The effects of target frequency in this paradigm were the focus of a separate paper [45].

During preliminary practice runs, the target difficulty was adjusted for each subject, for each visual field, so that the detection task was difficult (and thus so that highly focused attention was required) with a criterion of 80–95% correct target detection. This titration was done by slightly changing either the contrast and/or the size of the dots. The resulting parameters were then used for both the ERP and PET runs.

2.3. PET and MRI acquisition and analysis

PET imaging and analysis was performed using standard ^{15}O water-bolus techniques and change-distribution analysis [8], as described in Woldorff et al. [44]. Briefly, there were 10 runs in each subject’s session—four attend-left, four attend-right, and two passive—performed in counterbalanced order. All subjects had high-resolution, T1-weighted, gradient-echo, 3D MRI scans (TR=33 ms, TE=7.9 ms, flip angle=25°). The functional PET data were spatially smoothed with an 8-mm full-width half-maximum (FWHM) spatial filter. *Z*-score PET images of regional cerebral-blood-flow (rCBF) changes were overlaid on the MRI images from the same subjects, both for individual subjects and for the grand-averages.

2.4. ERP recordings and analysis

ERPs were recorded in a separate session of 40 runs (16 attend-left, 16 attend-right, and eight passive) from 64 electrode sites. Prior to the recording session, the positions of all the electrodes and of several fiducial skull landmarks were determined using a sonic-based 3D digitizer. The EEG channels were continuously recorded (sample rate per channel=400 Hz, bandpass=0.01–100 Hz), including several channels for monitoring and recording eye movements for later artifact rejection. ERPs to the standard and target stimuli under the various attention conditions were extracted by selective averaging, and attentional difference waves were calculated. Repeated-measures analyses of variance (ANOVAs) of the mean amplitude of ERP components across specified latency ranges were performed. Spherical-spline interpolation [33] was used to generate

scalp topographies of the ERP activities and attentional difference waves. Source analysis was performed on the attentional difference waves, constrained by seeding with PET activation foci, using the BESA (Brain Electrical Source Analysis) program [36] (see below).

2.5. Reference-frame co-registration

In order to accurately combine the data sets from the several imaging methodologies used here, including for performing the PET-seeded ERP source analysis, accurate co-registration of the various reference frames needed to be performed.

The ERP electrode locations for each of the subjects were first placed in a common reference frame based on the locations of the fiducial landmarks (the nasion and the left and right post-auricular points). To most accurately calculate topographic distributions or source analyses of the grand averages, the locations of the electrodes in this reference frame were then averaged across subjects (mean standard deviation of these locations across electrodes= 5.5 ± 3.0 mm).

The MRI and PET images were co-registered to each other and spatially normalized into the standard Talairach space [39] using the SN program [19]. The ERP electrode locations also needed to be co-registered with the Talairach reference frame so as to achieve correspondence with the PET activations and the MRIs, both for seeding purposes and for evaluating the locations of the final dipole location solutions. This was accomplished by using the relative locations of several head landmarks in the different reference frames. More specifically, for each MRI, the subjects had ear molds custom fit to their ears, and a small oil-filled, MR-visible capsule was pushed down into each. These fiducial locations and the nasion were thus easy to find in the MRI images. During the head digitization preceding the ERP session, the subjects wore the same ear molds, and these two points and the nasion were included as digitized points.

The transformation was accomplished using the 'hat-on-the-head' transformation from Pelizzari et al. [32]. More specifically, an image-processing program was used to extract the scalp from the MRIs, which were used as the 'head', and the electrode position files were converted to a 'hat' format. The Pelizzari-type program was then used to achieve a best-fit between the electrode positions and the scalp for each subject. To check the accuracy of the transformation of digitized electrode locations into MRI space, the inferred transformation function was then applied to the ear-mold and nasion locations in ERP-digitizing space (which were not used in the fitting routine). The transformed locations of these in the MRI space could then be compared to the actual locations of these fiducials in that space to check the validity/accuracy of the transformation. The average distance between the transformed and actual locations of these three points was $\sim5\pm2$ mm, indicating that reasonably accurate transformations had been achieved. The hat-on-the-head-transformed locations were then transformed into Talairach space and averaged together, as described above. These locations were the final ones used in the topographic plotting and source analyses of the ERP data.

2.6. ERP source analysis

ERP source analysis was performed on the attentional difference waves using the BESA dipole modeling software [36]. This program places dipoles in a simulated head, and iteratively adjusts their locations and orientations to achieve the best fit between the observed scalp potential distributions and the distributions the model dipoles would produce. This approach can be facilitated by the use of additional information [9], which in this study consisted of the PET activation foci, the locations of which were used in some of the analyses to seed (i.e. to begin) the source analysis iterations.

To perform the dipole source analysis using BESA, the grand-averaged, spatially normalized electrode locations in Talairach space (obtained as described above) were fed into BESA along with the Talairach-space PET activations. This then enabled the final BESA dipole solutions to be output into Talairach space as well.

The modeling of the ERP attention effects was performed in several different ways. One involved using the PET activation foci as a priori constraints on the source analysis. This can facilitate the source analysis by adding additional external information, but it does not have the benefit of independent comparison, nor of exploring more detailed spatial–temporal activation models. We also therefore used the approach of releasing the location constraints in the source analysis to explore the relationships between the independently obtained hemodynamic and electrophysiological data sets—i.e. the locations of the observed PET activations and the modeled generators. More specific descriptions of these analyses are given in the appropriate Results sections.

3. Results

3.1. ERP attention effects on non-targets

Fig. 2 shows the grand-averaged ERP responses at the 64 scalp sites as a function of attention condition for the standard (i.e. non-target) stimuli. The earliest-latency effect of attention on the ERPs was an enhanced positivity from 90 to 160 ms over occipital areas relative to passive. As reported in Woldorff et al. [44], which focused on the effects at the *peak* of the P1 wave, this 'early positivity' attention effect was significantly larger contralateral to the direction of attention.

A key, previously unreported, finding of the present report is that this early positivity attention effect was

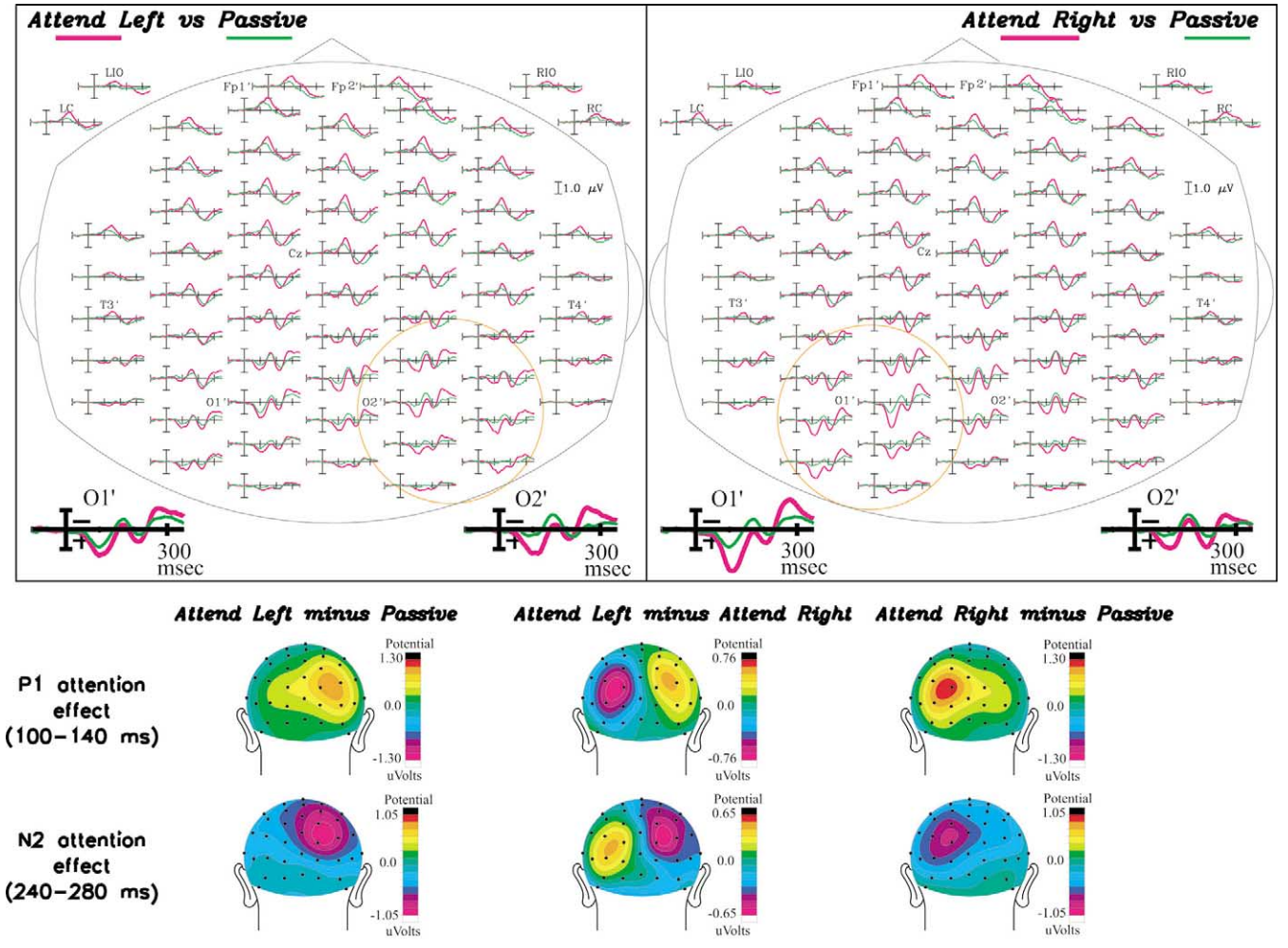

Fig. 2. ERPs as a function of the direction of attention, grand-averaged across subjects. Top, traces show the ERPs across the scalp to the bilateral standard (i.e. non-target) stimuli during the attend-left (left, top) and attend-right (right, top) conditions, each superposed on the ERPs to these stimuli during passive viewing; also shown in magnified view are these effects at a left and a right occipital scalp site (O1′ and O2′). Note that the P1 and N2 attention effects, at ~120 and 260 ms, respectively, are both larger contralateral to the direction of attention. Middle and bottom, topographic distributions of the grand-average ERP difference waves derived from the attend-left-minus-passive, attend-right-minus-passive, and attend-left minus attend-right subtractions, showing the effects of lateralized attention during the P1 and N2 latency ranges. Note the similar distributions of the P1 and N2 attention effects (especially for the attend-left vs. attend-right subtractions), although with opposite polarities.

followed later in the epoch by an attention-related enhanced negative wave (N2 effect, 220–280 ms) (Fig. 2). This enhanced negativity was also larger contralateral to the direction of attention, such that there also was a highly significant two-way interaction of attention direction× hemisphere ($P<0.001$).

Fig. 2 shows the topographic distributions of the attend-left-minus-passive (left column) and the attend-right-minus-passive (right column) subtractions around the peak of the P1 and around the peak of the N2. As can be seen in the figure, these attention effects, although of opposite polarity, had very similar distributions on the scalp. That is, these data show that sustained attention toward one side of a bilateral stimulus results in an enhanced positive wave predominantly over the contralateral occipital cortex at the P1 latency (100–140 ms) and an enhanced negative wave (N2 effect) peaking over essentially the same contralateral occipital scalp locations around 140 ms later (240–280 ms).

Fig. 2 (middle column) also shows the topographic scalp distribution for the subtraction of attend-left minus attend-right, which subtracts out any non-specific effects, such as arousal. For both the P1-latency and N2-latency effects, this subtraction yielded distributions having two focal peaks of opposite polarities over the two occipital cortices. Note again the very similar distributions of the P1 and N2 attention effects, but with opposite polarities.

Time-sequence topographic maps for the attend-left minus attend-right subtraction across the entire ERP epoch with 20-ms bin resolution are shown in Fig. 3. This shows the rise and decay over time of the contralateral attentional enhancements over the occipital cortex, revealing in great detail the temporal flow of the attention-enhanced processing in the brain.

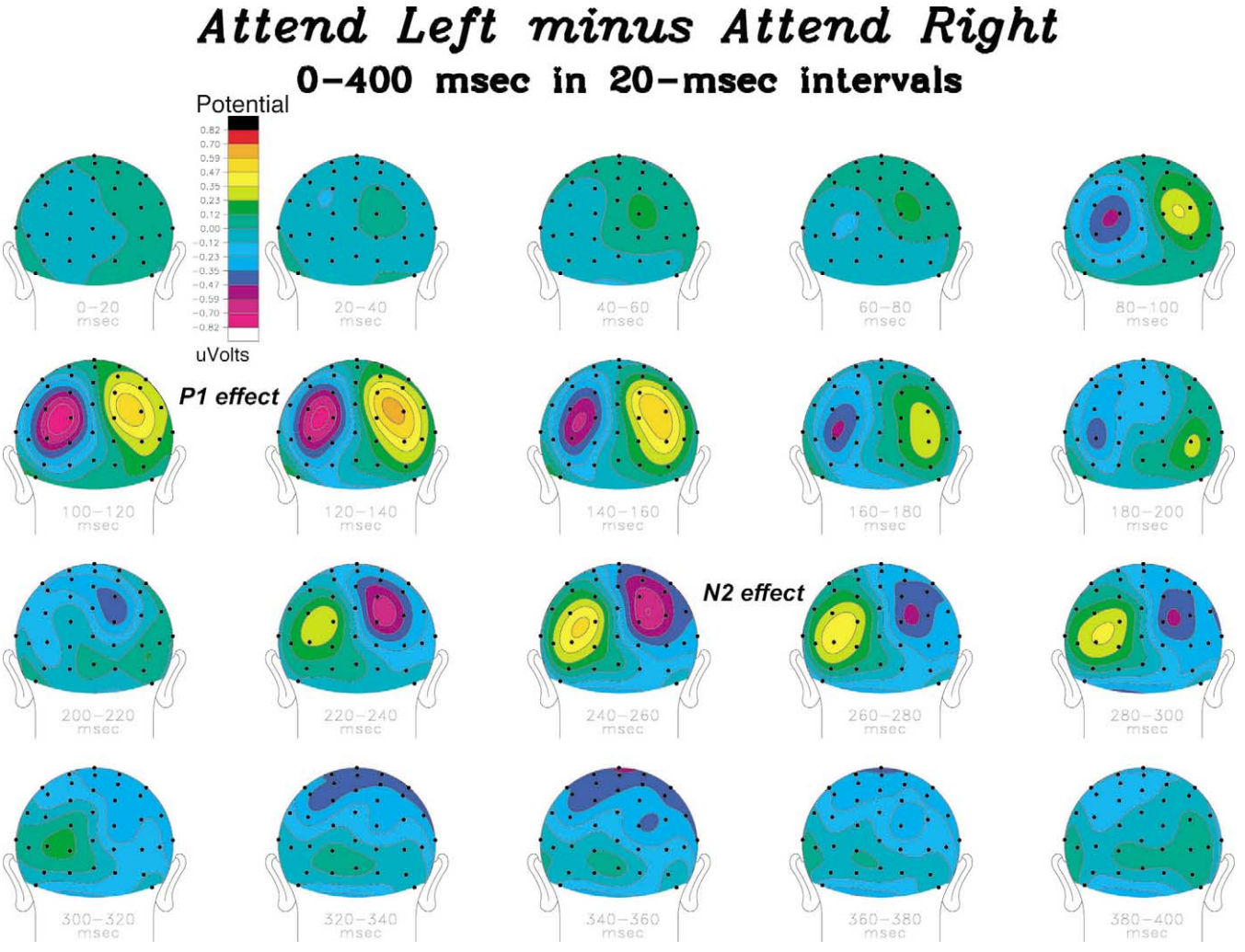

Fig. 3. Time-sequence topographic maps for the attend-left-minus-attend-right subtraction for the bilateral standards across the entire ERP epoch of 0–400 ms in 20-ms bins, showing the rise and decay over time of the contralateral attentional enhancements in occipital cortex.

3.2. PET attention effects

Fig. 4 shows the grand-averaged *z*-score horizontal PET images overlaid on the grand-averaged structural MRI images from the same subjects at two levels of occipital cortex. Fig. 4 (top) shows that the active attention conditions relative to the passive condition elicited particularly strong activity in the contralateral *dorsal* occipital areas (Brodmann Areas (BA) 18/19), as previously reported in Woldorff et al. [44]. In addition, substantial, albeit lesser, activation was seen in the contralateral ventral occipital cortex (fusiform gyrus, BA 19) (Fig. 4 (bottom)).

There were various activation increases and decreases throughout the brain that were in common between the attend-left vs. passive and attend-right-vs.-passive contrasts, with little or no tendency toward contralaterality (e.g. parietal cortex, anterior cingulate—not shown). These effects therefore subtracted away in the attend-left-vs.-attend-right contrast, leaving a simpler distribution of activations. More specifically, the main attention-related foci remaining in the attend-left-vs.-attend-right contrast were the activation of contralateral dorsal occipital (DO) cortex and the smaller effect in ventral occipital cortex, as seen in Fig. 4.

It is important to note that the PET effects in the DO cortex were particularly large in extent, with total cluster sizes of 1600–2400 mm^3, suggesting that these effects probably covered more than just a single functional area. At their most inferior and medial point, the dorsal occipital effects started around 1 cm above the calcarine sulcus, indicating that there was no significant attention effect in V1 (striate cortex). However, at least in the attend-left minus attend-right subtraction, these effects extending as close as 1 cm from the calcarine suggests that they probably did include V2. From there, the activated area extended superiorly, anteriorly, and laterally. The extent of

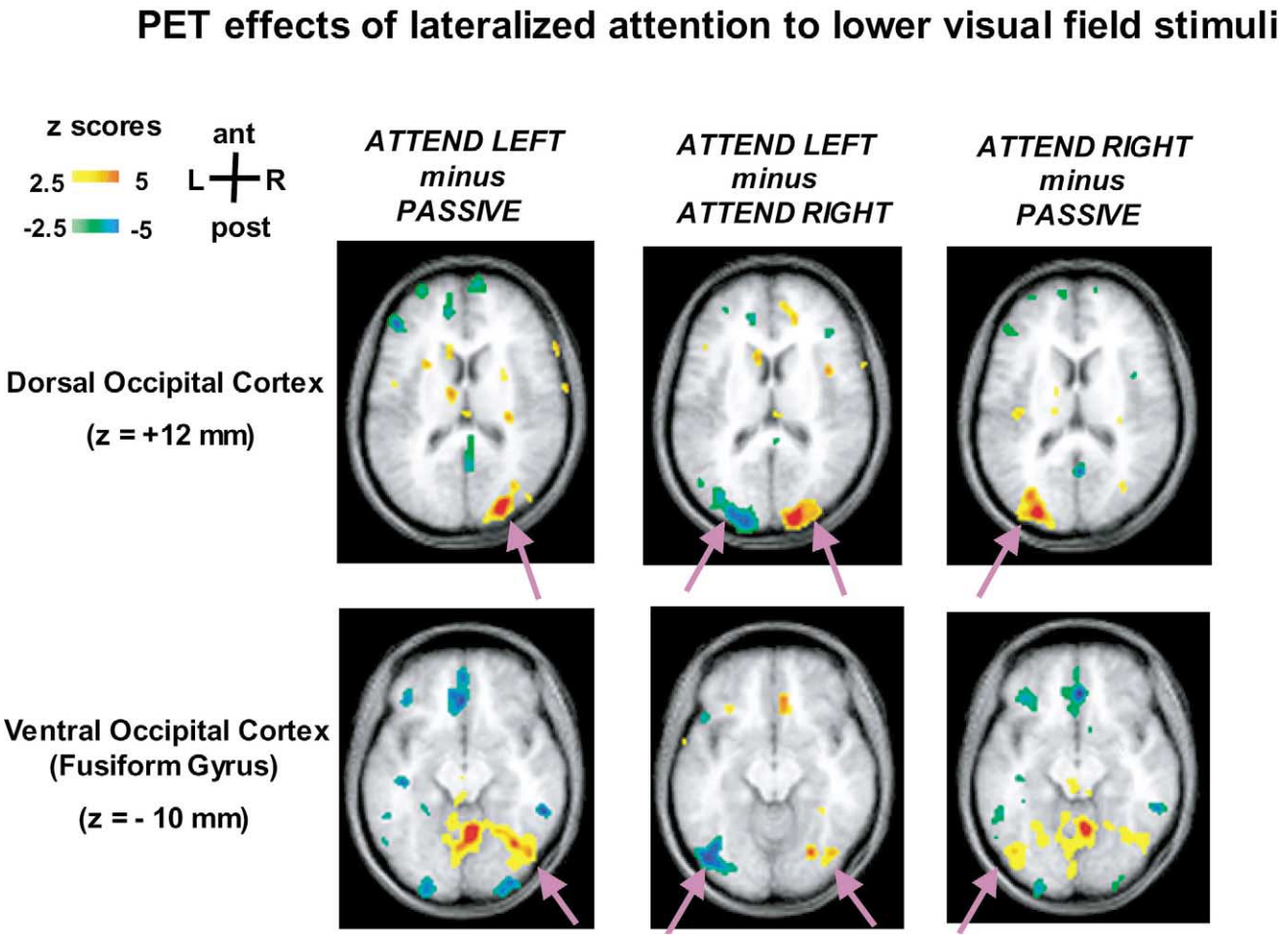

Fig. 4. Grand-averaged *z*-score PET difference images (axial) showing the effects of lateralized visual attention at two levels of occipital cortex: dorsal (Talairach $z = +12$) and ventral (Talairach $z = -10$; fusiform gyrus). The PET activity maps are shown overlaid on the grand-averaged structural MRI images from the same subjects. As with the ERPs in Fig. 2, the contrasts shown are for attend-left vs. passive, attend-right vs. passive, and attend-left vs. attend-right. Note the particularly strong activity in the *contralateral dorsal occipital areas* (Brodmann Areas (BA) 18/19) (top) with some, but lesser, activation in ventral occipital cortex (bottom).

the activation was greater on the left, especially in the medial-to-lateral dimension, which can be seen in Fig. 4.

3.3. ERP source modeling

The contralateral attention-related occipital PET activation and the contralateral ERP effects appeared to be experimentally associated. However, to draw tighter connections between these hemodynamic and electrical changes required a modeling analysis. First, it was important to evaluate whether the PET activation areas were viable candidates as sources for the electrical effects. Moreover, for the focus of this paper, it was of interest to ascertain whether activity at different latencies in the ERP attention effects could be mapped to different portions of the extended PET attention-related activation foci.

To address these questions, PET-seeded, iterative, dipole source modeling using BESA was applied to the attend-left-minus-attend-right ERP difference waves. These difference waves were the best to use for our modeling purposes, in that non-specific effects, such as effects of arousal, were eliminated in this subtraction, therefore yielding distributions that were both simpler and that focused on the effects of *selective* attention. In addition, the analogous attend-left-vs.-attend-right subtraction in the PET data correspondingly reduced the number of likely candidate dipole sources, in that there were considerably fewer activation foci in this hemodynamic contrast relative to the contrasts of the active-attend conditions vs. passive.

3.3.1. P1 effect (peak)

As reported in Woldorff et al. [44], two dipoles constrained to the centroids of the two DO PET foci (left: $x = -28$, $y = -89$, $z = +6$; right: $x = +18$, $y = -91$, $z = +12$), with only orientation of the dipoles being allowed to vary, yielded an excellent fit to the distribution at the *peak* of the P1 attention effect (2.5% residual

variance, or RV). When locations of the dipoles were also allowed to vary, the dipoles moved slightly anteriorly and laterally, and explained all but 1.6% of the P1 *peak* effect. In contrast, dipoles constrained to the ventral occipital PET foci (i.e. fusiform gyrus: left: $x = -45$, $y = -71$, $z = -9$; right: $x = +26$, $y = -75$, $z = -11$) provided a rather poor fit (16% RV) for the P1 effect. When location was also allowed to vary, the dipoles moved upward during the iterative dipole fitting, stabilizing again in the DO locations. As argued in Woldorff et al. [44], this modeling behavior strongly suggests that the DO PET locations contained the major contributing source or sources at the peak of the ERP P1 attention effect.

3.3.2. N2 effect (peak)

The later N2-latency attention effect peaking at around 250 ms had a very similar distribution as that of the P1 effect (Fig. 2, bottom). Such similarity was further demonstrated by the equivalent modeling behavior of the P1 and N2 attention effects. More specifically, just like for the P1 effect, PET-seeded dipoles placed in the DO area also fit the N2 attention effect quite well (orientation only fit: 3% RV; full fit: 2% RV; see Fig. 5). In addition, also like the P1 effect, the N2 effect was *not* well modeled by dipoles in the ventral occipital locations (RV=12%). These combined findings strongly suggest that this longer-latency electrophysiological effect reflects *re-entrant* attention-related activity at the same dorsal occipital location showing enhancement at the earlier P1 peak time.

It should be noted that adding more dipoles for the modeling analysis to the two in DO cortex did not improve the solutions for either the P1 or N2 effects. More specifically, additional dipoles placed in either the fusiform PET foci or, for that matter, anywhere else in the brain, resulted in little change in the residual variance of the solutions relative to the DO ones alone.

3.3.3. Modeling the spatial temporal activation patterns across time

In the above modeling, the attention effects at the peaks of both the P1 and N2 were well modeled as arising from the contralateral dorsal occipital areas shown to be activated in the parallel PET experiment. However, thus far this mapping between the ERP and hemodynamic activations has focused on modeling each of these ERP attention effects at its peak and discovering that it mapped well to a single location—or, in this case, a bilateral pair of locations—in the PET, namely the centroids of the parallel PET focus. As clearly seen in Fig. 3, the ERP tracings showed a dynamic sequence of attention-related effects extending across a protracted *time* period. Similarly, as noted above, the PET activations in dorsal occipital cortex had a substantial *spatial* extent, presumably covering several of the specific early visual functional areas. It would seem highly unlikely that attention-induced enhancement in these several areas would all occur at exactly the same latency. However, from the PET data alone it is not possible to infer anything about the timing or the temporal sequence of activations in this cluster of activations.

Thus, in order to clarify the relationships between the spatial–temporal patterns of the attention-related ERP

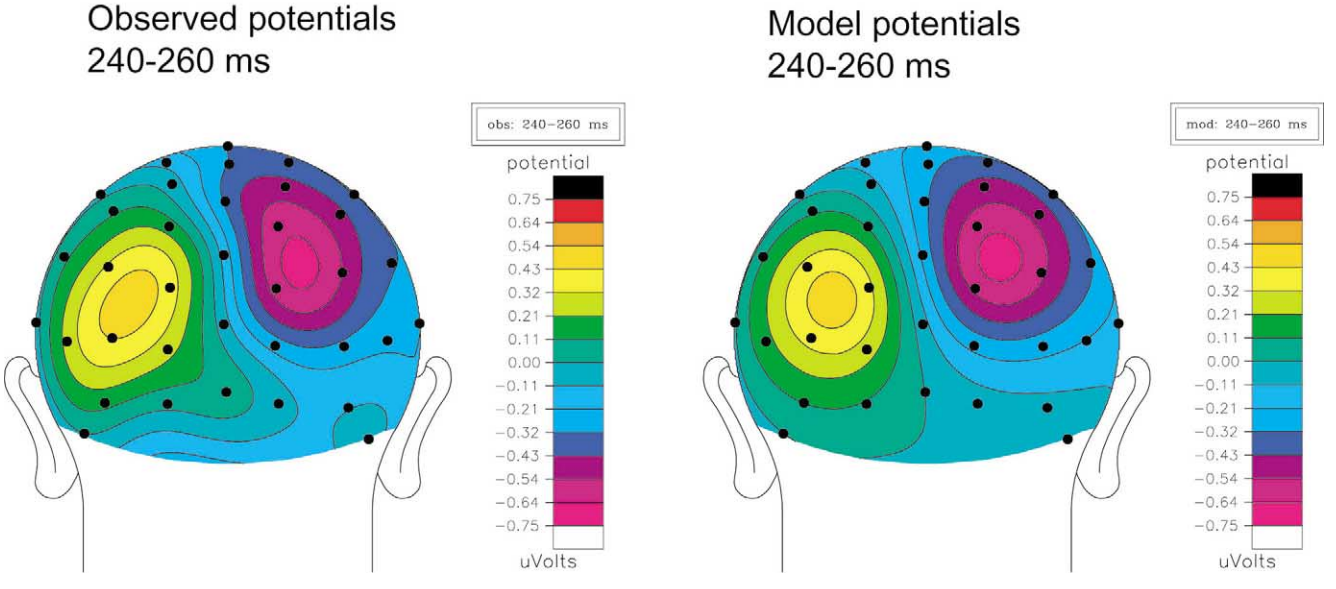

Fig. 5. Dipole fit for the attention effect (attend-left vs. attend-right) for the bilateral standards at the peak of the N2 (240–260 ms). (Left) Observed potentials of the attention effect during this time window. (Right) Model potentials for this distribution, seeded by PET foci in the left and right dorsal occipital (DO) cortex. Using two dipoles constrained to the PET DO foci, the difference between the observed and the model distributions was ~3% residual variance. After the location constraints were released (but still allowing orientation to vary), the dipoles moved slightly (~0.5 cm), and the RV reduced to ~2%.

activity and the spatial pattern of PET activations, we performed more detailed modeling of these attention effects across time. In particular, we first examined the fits across time using the DO dipole pair, looking at how well this dipole pair could model the temporally extended ERP attention effects at successive 10-ms bins (Fig. 6). Seeding with the left and right DO PET activation centroids and letting only orientation vary (solid line) revealed the good fits at the peaks of the P1 and N2, as noted above (i.e. note the low residual variance at these latencies). However, releasing the location constraints in each of these 10-ms time bins (Fig. 6, dashed line) resulted in good fits being obtained across a much wider period around the P1 (90–160 ms).

This result raises the question as to how do these model dipoles move during this extended period to yield these fits—namely, whether they just move somewhat randomly around the occipital cortex, or rather they move in a systematic fashion that might reveal important spatio–temporal relationships, such as the sequential order of activation of extrastriate areas modulated by early visual attention.

Examination of the estimated locations of this pair of model dipoles indicated that they *do* appear to move systematically across the 90–160 ms time range, starting at the beginning of this time period at points that are at the most inferior, posterior, and medial regions of the PET DO activations (~1 cm dorsal to the calcarine) and then moving superiorly, laterally, and anteriorly (see Fig. 7). This movement thus roughly paralleled the shape of the PET activations in DO cortex. Furthermore, the similarity between the independently obtained hemodynamic and electrophysiological data sets also included the result that both dorsal occipital dipole and the dorsal occipital PET activation area in the left hemisphere had a much wider lateral extent and were somewhat more inferior than was the right dipole and the right PET activation area (compare Figs. 2 and 7).

In contrast to the P1 effect, releasing the location constraints across time did not substantially extend the time period in which good fits were obtained for the attention effect around the N2 latency. That is, the window around the N2 in which good fits were obtained was more temporally focal, being just near the peak of the wave. Thus, although this fit at the N2 peak was excellent (2% RV) and was consistent with a re-entrance of attention-enhanced processing in the same contralateral DO cortex, there was no clear evidence obtained for an analogous (or reversed) movement of the attention effect activation pattern during an extended time period leading up to the N2.

3.3.4. Target-related N2 effects (N2b)

At the P1 latency, lateralized-attention ERP effects in response to targets did not differ from those for non-targets (standards). However, differences emerged at longer latencies. More specifically, targets also elicited an enhanced N2 response ('N2b') that, like the standards, was larger

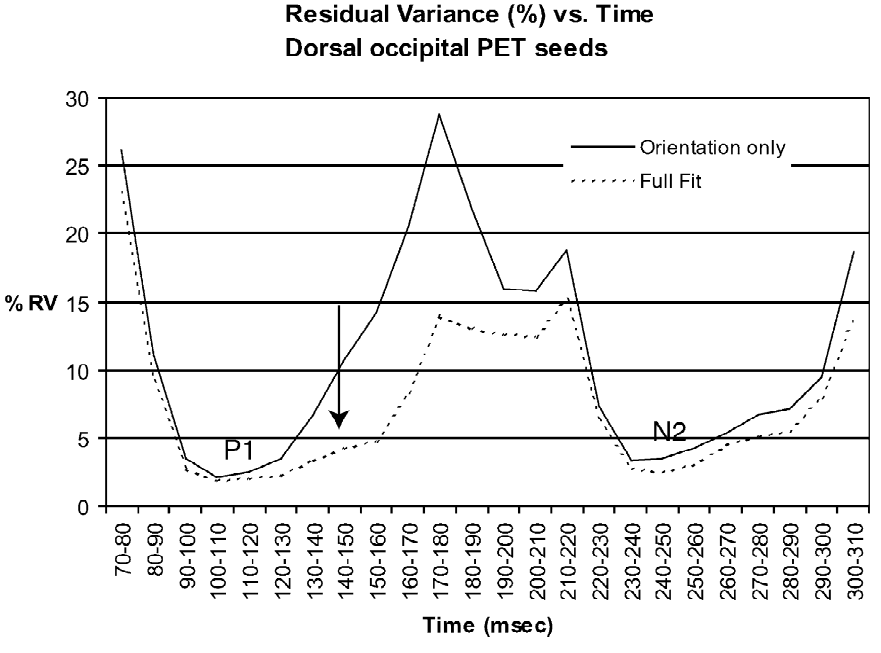

Fig. 6. Dipole fits of the attention effect across the ERP epoch. Displayed are the residual variance (RV) of the best fits across time, seeded with dipoles in the left and right dorsal occipital (DO) cortex, with the fits performed at successive 10-ms bins. Fits with the dipole pair constrained to the locations of the left and right DO PET activation centroids and letting only orientation vary (solid line) revealed the good fits at the peaks of the P1 and N2 (i.e. note the low RV at these latencies). Releasing the location constraints in each of these time bins (dashed line) resulted in good fits being obtained across a much wider period (arrow) around the P1 (90–160 ms).

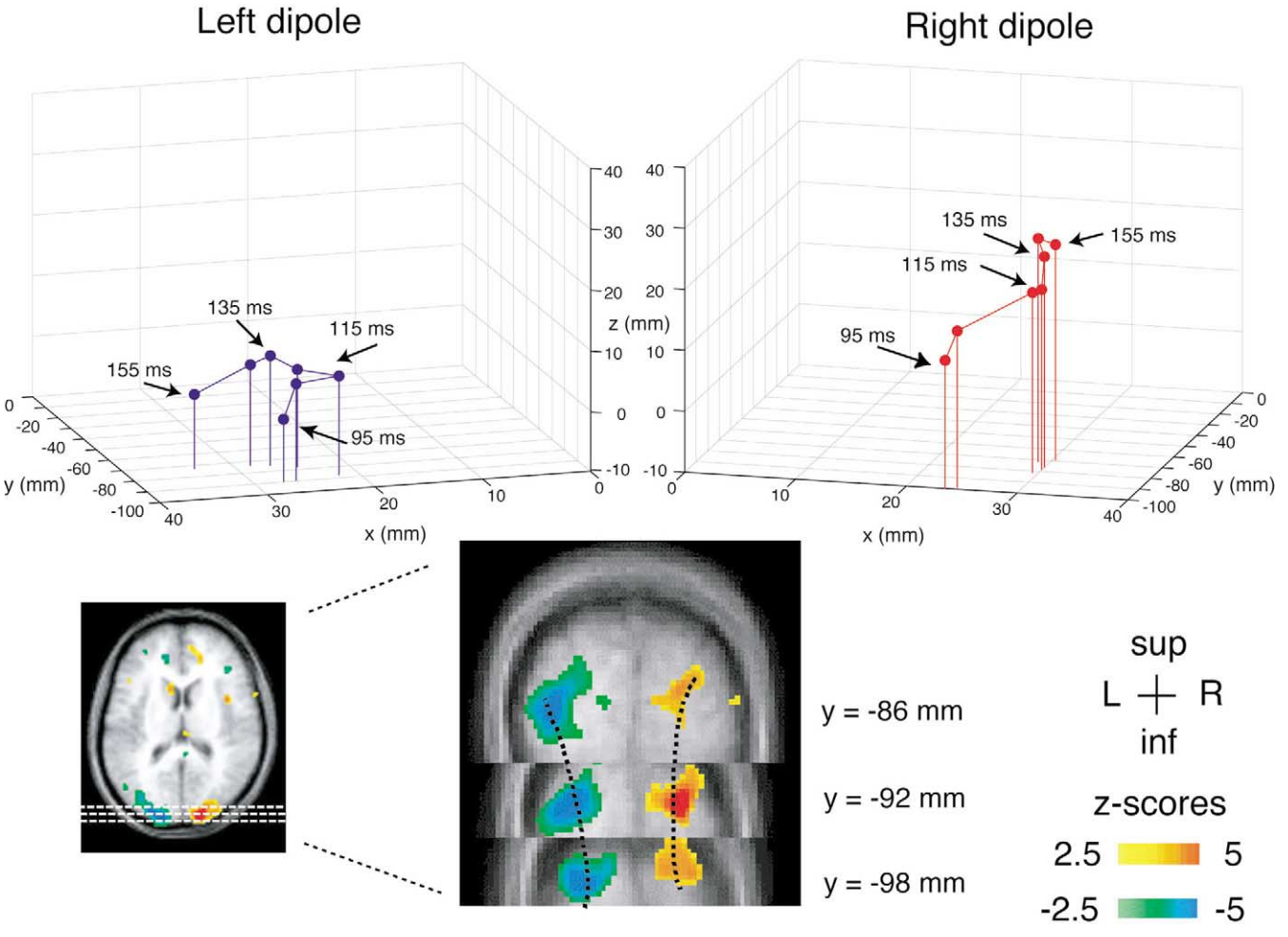

Fig. 7. Movement of the best-fit dipole pair in DO cortex for the attention effect across the wide period (90–160 ms) around the P1. Note the general movement of these dipoles dorsally, laterally, and anteriorly across this period. This apparent movement coursed through the DO PET activation areas, roughly paralleling their shape, and is interpreted as reflecting the average movement of the attention effect through the early, retinotopically organized, visual areas in DO cortex that represent the lower visual field (see text). Coronal views of the corresponding DO PET activations are also shown.

contralateral to the direction of attention, but this lateralized negative-wave enhancement was even larger than that for the standards (target-side×hemisphere×target/standard, $P<0.001$) (Fig. 8), and continued for a more prolonged period of time (240–440 ms). This contralateral target-related N2b effect was followed by, and partially overlapped by, the large, bilaterally distributed, parietal P3 wave typically associated with detected targets (Fig. 8).

The topographic distribution for the target-related N2b looked similar to the N2 attention effect for the standards (Fig. 8). To best isolate the distribution of the contralateral target-related N2b waves, the following double subtraction was performed. First, the left-attended and right-attended standard ERPs were subtracted from the corresponding left-attended and right-attended target ERPs, thereby isolating the contralateral target-related N2b and the succeeding P3 wave (Fig. 8, middle row). In these difference waves, however, the early part of the large amplitude, parietally distributed P3 partially overlapped with the occipital N2b, thereby tending to distort the scalp distribution of the latter. To remove the bilaterally distributed P3b, we performed an additional subtraction of the two above-described difference waves—i.e. [(left-attended-target) minus (left-attended-standard)] minus [(right-attended-target) minus (right-attended standard)]. As can be seen in Fig. 8 (bottom row), this double difference wave effectively cancelled out the target-related P3b effects, thereby more fully unmasking the contralaterally organized, occipital N2b effect for detected targets.

Source information of the target-related N2b was investigated by performing dipole source analysis on these double difference wave distributions, again first using as seeds the PET-derived DO cortex foci. This analysis revealed a relatively good fit for the contralateral N2b effect (7.4% residual variance at the peak), although not nearly as good as for the P1 and N2 effects for the standards. In addition, fits constrained by using the two *ventral* occipital PET foci alone were considerably worse (11%), similar to the result for the non-target P1 and N2, although not as poor as the fit in those cases when using

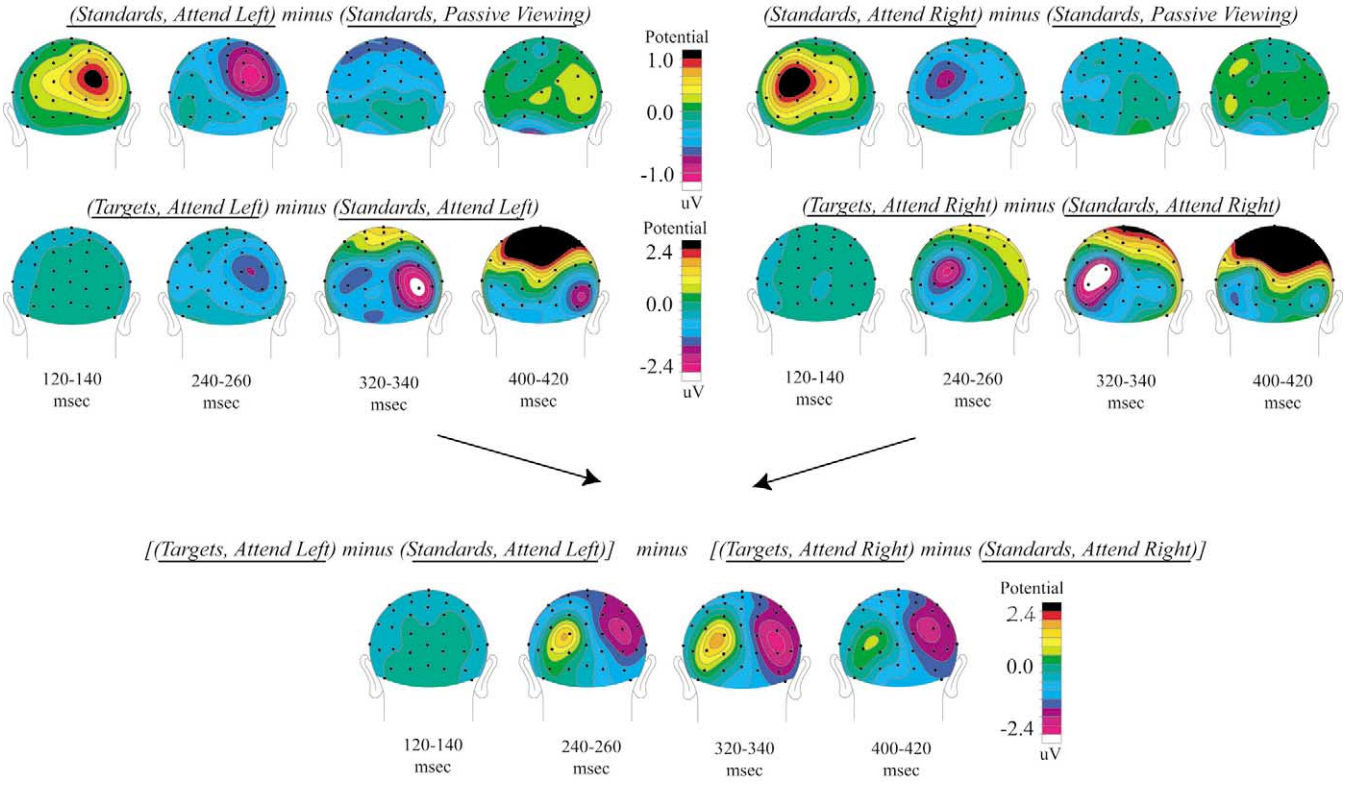

Fig. 8. Topographic plots of the difference waves isolating the target-related occipital N2b activity. Top row, difference of ERPs to the bilateral standards when attending to the left or right minus when passively viewing them, shown at several time windows. Middle row, difference of ERPs to the attended-left or attended-right targets minus the attended-left or attended-right standards, shown at the same time windows. Note the lack of difference in the P1 latency range (120–140 ms), due to the targets and standards *both* having enhanced contralateral P1 activity. Rather, the target-related difference begins during the N2 latency range (~240–260 ms) as an *additional* contralateral occipital effect. This effect, however, is soon distorted by the large-amplitude succeeding P3. Bottom row, double difference of the difference wave activity shown in the left and right sections of the middle row. This double difference subtracts out the large, bilaterally distributed P3 wave, better isolating the target-related occipital N2b activity. Source analysis of this activity distribution was performed for understanding target-related occipital processing (see text).

the ventral occipital foci. Moreover, in the case of the target-related N2b, *adding* the ventral occipital PET-derived foci to the DO foci for the source analysis considerably *improved* the fit (to 4.7% residual variance). In contrast to the P1 and N2 non-target source analyses, these patterns of modeling results suggest a possible contribution of the ventral occipital areas to the target-related N2b effects.

4. Discussion

The combined electrophysiological and hemodynamic results of this study provide a novel and compelling model of the spatial–temporal attention-related activation patterns in early, retinotopically organized, visual areas of occipital cortex. The PET results revealed that sustained spatial attention to the lower visual field gives rise to increased activity in an extended region of the dorsal occipital cortex (DO) contralateral to the direction of attention, while the ERP data showed enhanced electrical activity over the contralateral occipital cortex for an extended period of time beginning at 80 ms post-stimulus. Detailed source analysis of the P1-latency ERP attention effects (80–160 ms) revealed a movement of the P1-attention-effect model dipoles across the spatially extended PET DO activation region over this time period. This dynamic progression of the P1 attention effect suggests the sequential recruitment of different generators of P1 sub-components along the early retinotopically organized visual areas in the dorsal occipital cortex.

A second important and novel finding of this study is the empirical demonstration of attention-related *re-entrant* activation (N2 window: 240–280 ms) of the same retinotopically organized region of contralateral dorsal occipital cortex that was active during the peak of the earlier-latency P1 attention effect (80–140 ms). Lastly, while contralateral *dorsal* occipital cortex appears to be critical in the early spatially selective attentional gating of portions of bilaterally presented lower-visual-field stimuli, our results also provide evidence that *ventral* occipital cortex may also be selectively (and dynamically) recruited upon correct target discrimination at the attended lower visual field location.

4.1. Spatial–temporal relationships between P1-latency attention effects and early visual areas in dorsal occipital cortex

The PET data indicated that sustained visual spatial attention to lower visual field stimuli elicited strong enhancement of activity in the contralateral dorsal occipital cortex. These effects were fairly large in extent, covering at least several of the early lower-field visual areas in this region. Because these effects occurred within about 1 cm of the calcarine sulcus (from above), but did not include it, we infer that the effects of the attentional manipulation probably included dorsal V2, V3, V3a, representing the lower visual field [11], but did not include the primary visual cortex, V1.

As previously reported [44], the P1 ERP attention effect peaking at 120 ms was well modeled with a dipole seeded with the centroids of the DO PET attention effects. However, as noted above, the large spatial extent of DO cortex PET activations likely reflected attention-related enhancement in *several* of the early lower-field visual areas rather than just one. In addition, the ERP attention effects were more protracted across time than just a very sharp transient enhancement around 120 ms. The additional modeling reported here sheds light on the spatial–temporal relationships between these ERP and PET attention-related activations.

More specifically, further dipole modeling in the DO activation region across the 90–160 ms range suggests that the P1 attention effect is actually composed of a series of subcomponents that reflect the sequential activation of attention-induced processing enhancement of several of the early lower-field visual areas (e.g. first V2, then V3, V3a, etc.), consistent with the dynamic spatio–temporal flow of attention-enhanced activity through the DO cortex. Note that our proposed model is not that there is neural activity 'sliding' in a continuous manner across time along the cortical surface that contains these various visual areas. Rather, we interpret our results to mean that these early discrete visual areas have somewhat different temporal onsets of attention-enhanced activity, partially overlapping in time, and that modeling these effects with only one dipole on each side gives an *apparent* movement across the dorsal occipital volume. However, we propose that this model-dipole movement actually reflects, at least in a centroid sense, the average spatial–temporal flow of attention-enhanced activity in the early visual sensory areas, beginning at V2. In support of this proposition are the results that an unconstrained dipole pair fit very well to the observed data across this entire latency period (90–160 ms); that the dipole movement paralleled the shape of the PET activation patterns in this area; and that the latter PET activated region covered the known spatial layout of the hierarchy of the early visual lower-visual-field sensory areas (V2, V3, V3a) [2,10,37,41]. In addition, previous studies have suggested that the time range of 60–90 ms is dominated by V1 activity, and that extrastriate activation begins at the later part of this range [3,22]. Thus, the onset of the attention effect in the present experiment being at 80–90 ms (see Fig. 2) is quite consistent with the initial part of the effect reflecting attention-enhanced V2 activity *in the first initial volley through V2*, which was then followed by the ramifications of these attention effects through the succeeding levels of the early visual sensory areas.

4.2. Re-entrance of activity in the dorsal occipital cortex: the contralateral N2 attention effect

These data also provide novel evidence for re-entrant attention-related activation in the same lower-field area in the dorsal occipital cortex. The topographic distribution of the contralateral N2 attention effect at 250 ms was strikingly similar to that of the earlier-latency P1 effect, and source analysis indicated that the DO areas were likely to be a major source for this later effect as well. Indeed the dipole fit for the N2 effect using these source locations was as good as that for the P1 effect itself.

Other evidence for attention-related re-entrance to V2 and other extrastriate visual areas comes from a recent electrophysiological study in monkeys by Mehta et al. [28]. These authors showed that effects of visual attention occurred later in V2 than in the higher-level visual area V4. They concluded that the return of activity to V2 was perhaps due to re-entrant input from V4 or other higher areas. Thus, this late effect in V2 in monkeys may be related to the attention effects in V2–V3 in the present study. However, one key difference between that study and the present one is that in the present study there is an *early* effect of attention in V2, followed by attention effects in higher-level areas, then followed by a return of attention-related activity in V2 again. Task- and species-related differences between Mehta et al. and the present study may account for the difference in early attentional enhancements in V2–V3 prior to the higher level attention effects observed in the two studies.

Hemodynamic studies of visual imagery and visual attention have provided evidence for top-down modulation of activity in early sensory areas, by showing activity as early as striate cortex [18,37]. However such techniques cannot provide any information about the timing characteristics of such effects.To our knowledge, the present study provides the first empirical evidence to date, that top-down attentional control results in *re-entrant* activity in this same retinotopically organized region of early extrastriate visual cortex that is the site of the first pre-set attentional modulation of neural activity (P1).

A key point here is that the present findings indicate that re-entrant activations of early visual cortex during focused selective attention are *also retinotopically organized*. The N2 enhancement effects were best modeled by dipoles in contralateral DO cortex, which is where the lower visual

field is represented in early visual cortex and was also the same region of the early, preset attentional modulation of the P1 for lower-field visual stimuli. Moreover, the excellent source analysis fit (~2% residual variance) of both the P1 and N2 attention effect for the standards with locations in DO cortex only (with little fit improvement by adding more dipoles in ventral occipital cortex or elsewhere) suggests that neither the early nor the late re-entrant effect of sustained attention for the non-target standards trigger significant activity in the ventral occipital cortex.

4.3. Target-related N2 effects

Another result of this study is that correctly detected targets elicited additional late negative-wave activity. It is important to note that this target-related 'N2b' activity, which was also contralaterally distributed, was *in addition to* the enhanced contralateral negativity that was elicited by all the attended stimuli, including the standards. (Recall that the isolation of the target-related N2 included the subtraction of the responses to targets minus standards for the same attention condition, which thereby subtracted out the contralateral N2 attention effect that was already present in the standards.) The comparison of the N2 effects elicited by the standards and the additional N2 activity specific for the targets revealed some interesting differences that may provide insight into the functional roles of these activations. More specifically, the N2 attention effects for the standard stimuli were very well modeled by sources only in DO cortex, with no additional apparent contribution of a source in VO cortex, whereas the N2b target-related effects were best modeled when a second pair of dipoles were placed in VO cortex. Furthermore, target-specific N2 effects peaked somewhat later than the N2 effect on the standards, and were considerably more protracted in time.

The N2b effects for attended targets in the present experiment may be related to the 'N2pc' component (180–280 ms) elicited by contralateral *target* stimuli within a bilateral stimulus array [20]. It may be important to note that the MEG analogue of the 'N2pc' to targets (collapsed across upper and lower visual fields) has been modeled as arising in part from the contralateral ventral occipital cortex (fusiform gyrus) [16].

The pattern of N2 results for the standards and the targets obtained in the present study suggests the following interpretation of these longer-latency effects: top-down control of highly focused sustained attention to *all stimuli* in the *lower visual field* results in the re-entrant activation of the retinotopically correspondent contralateral DO cortex (which also gave rise to the earlier-latency P1 attention effect). During this N2 time period, as a target in the attended location of the lower visual field is detected, still additional re-activation of DO cortex occurs, over and above that for the standards in both amplitude and duration. In addition to this ongoing enhanced activity in DO cortex, the need for target analysis appears to result in the additional recruitment of contralateral VO cortex. This recruitment of VO cortex may be related to it being a substrate of shape/object recognition [42,43]. More specifically, this concurrent activation of VO cortex for the targets during this time may reflect the accrual of target-related information that is being sent to the ventral stream (perhaps from DO cortex in this case) for further object-related analysis. If so, then the stimuli in the present experiment not being very object-like might explain why the activation in VO was not very strong here, but perhaps would be under other circumstances requiring more sophisticated object analysis. Further research is required to specifically test this hypothesis.

4.4. Attention and V1

The current study provides no evidence for an effect of attention in V1 in either the ERP or PET data. The lack of an *early* effect in V1 in the ERP data (i.e. on the initial volley through striate) is consistent with various previous ERP studies looking for, and not finding, early V1 effects [3,22,23,26]. On the other hand, various recent neuroimaging studies using fMRI have reported hemodynamic effects of attention in V1 (e.g. Refs. [2,26,30,41]). Moreover, the multimethodological Martinez et al. [26] study, also employing a lateralized spatial attention task, reported hemodynamic (fMRI) attention effects in V1, despite not observing an early V1 ERP effect in the same task in the same subjects. The fact that a V1 hemodynamic effect was observed in Martinez et al. [26] but not here may be related to the use of distractors in that experiment. Such a result would be consistent with the view that attentional modulation at the level of V1 is necessary when it is required to 'filter out' closely located distractors in the visual field [29].

In Martinez et al. [26], the presence of an attention effect in the fMRI but not in the early ERPs led the authors to speculate that this resulted either from the attention effect in V1 being sustained across time (thereby being reflected in the block-design fMRI data but not in the transient electrophysiological responses) or from the effect being late and re-entrant (and not observed because it was masked by other, larger, late attention effects). A later report by the same group [27] provides a source analysis model consistent with such a late attention effect in V1. The view suggested here is that re-entrance of attention-enhanced processing back to early visual areas—observed in the Martinez et al. experiments and in the present experiment—is a common and/or basic mechanism important in selective attention. As mentioned earlier, we hypothesize that the reason re-entrance may have occurred all the way back to V1 in Martinez et al. [26] and not in the present study may be related to the presence of closely placed distractors in the visual field in the former. New strong evidence for attention-related re-entrant activity all

the way back to V1 for target stimuli in a spatial attention task involving distractors is also provided by a recent study by Noesselt et al. [30] using combined fMRI, MEG, and ERPs.

In summary, the present combined ERP/PET study indicates that lateralized visual spatial attention results in a preset biasing of the early, extrastriate, visual sensory areas in a retinotopically organized way. In the present experiment involving attention within the lower visual field, these effects occurred in the contralateral dorsal occipital cortex, where the lower visual field is represented. This enhanced neural activity resulted in enhanced contralateral ERP activity across 90–160 ms, which appeared to reflect the attentional modulation of the initial sequence of activation of the sensory stimulus processing in these areas, beginning as early as V2 at about 90 ms in the present paradigm. In addition, these effects were followed by a return or re-entrance of attention-enhanced activation (the N2 effect) to the same early visual areas at around 250 ms, perhaps to enable more specific focusing of processing of the stimuli in the attended channel (i.e. in the attended region of space) for the purpose of target vs. non-target discrimination. Finally, detection or discrimination of targets in the attended stream of stimuli appears to elicit yet additional re-entrant activity in the retinotopically organized early visual areas, while also recruiting ventral occipital processing, which could possibly be related to object analysis.

Acknowledgements

This work was supported in part by NIMH grant MH60415 to M.G.W.

References

[1] P.A. Bandettini, A. Jesmanowicz, E.C. Wong, J.S. Hyde, Processing strategies for time-course data sets in functional MRI of the human brain, Magn. Reson. Med. 30 (2) (1993) 161–173.
[2] J.A. Brefczynski, E.A. DeYoe, A physiological correlate of the 'spotlight' of visual attention, Nat. Neurosci. 2 (4) (1999) 370–374.
[3] V.P. Clark, S. Fan, S.A. Hillyard, Identification of early visual evoked potential generators by retinotopic and topographic analyses, Hum. Brain Mapp. 2 (1995) 170–187.
[4] M. Corbetta, S. Miezin, S. Dobmeyer, G.L. Shulman, S.E. Petersen, Selective and divided attention during visual discriminations of shape, color, speed: functional anatomy by positron emission tomography, J. Neurosci. 11 (1991) 2383–2402.
[5] M. Corbetta, G.L. Shulman, Control of goal-directed and stimulus-driven attention in the brain, Nat. Rev. Neurosci. 3 (2002) 215–229.
[6] A.M. Dale, E. Halgren, Spatiotemporal mapping of brain activity by integration of multiple imaging modalities, Curr. Opin. Neurobiol. 11 (2) (2001) 202–208.
[7] A.M. Dale, A.K. Liu, B.R. Fischl, R.L. Buckner, J.W. Belliveau, J.D. Lewine, E. Halgren, Dynamical statistical parametric mapping: combining fMRI and MEG for high-resolution imaging of cortical activity, Neuron 26 (1) (2000) 55–67.
[8] P.T. Fox, M.A. Mintun, E.M. Reiman, M.E. Raichle, Enhanced detection of focal brain responses using inter-subject averaging and change-distribution analysis of subtracted PET images, J. Cereb. Blood Flow Metab. 8 (1988) 642–653.
[9] P.T. Fox, M.G. Woldorff, Integrating human brain maps, Curr. Opin. Neurobiol. 4 (2) (1994) 151–156.
[10] M.K. Hasnain, P.T. Fox, M.G. Woldorff, Intersubject variability of functional areas in the human visual cortex, Hum. Brain Mapp. 6 (4) (1998) 301–315.
[11] M.K. Hasnain, P.T. Fox, M.G. Woldorff, Structure–function spatial covariance in the human visual cortex, Cereb. Cortex 11 (8) (2001) 702–716.
[12] H.J. Heinze, S.J. Luck, G.R. Mangun, S.A. Hillyard, Visual event-related potentials index focused attention within bilateral stimulus arrays. I. Evidence for early selection, Electroencephalogr. Clin. Neurophysiol. 75 (6) (1990) 511–527.
[13] H.J. Heinze, G.R. Mangun, W. Burchert, H. Hinrichs, M. Scholz, T.F. Muente, A. Gos, M. Scherg, S. Johannes, H. Hundeshagen, M.S. Gazzaniga, S.A. Hillyard, Combined spatial and temporal imaging of brain activity during visual selective attention in humans, Nature 372 (1994) 543–546.
[14] S.A. Hillyard, G.R. Mangun, M.G. Woldorff, S.J. Luck, Neural systems mediating selective attention, in: Handbook of Cognitive Neuroscience, MIT Press, Cambridge, MA, 1995, pp. 665–681.
[15] S.A. Hillyard, T.F. Munte, Selective attention to color and location: an analysis with event-related brain potentials, Percept. Psychophys. 36 (2) (1984) 185–198.
[16] J.M. Hopf, S.J. Luck, M. Girelli, T. Hagner, G.R. Mangun, H. Scheich, H.J. Heinze, Neural sources of focused attention in visual search, Cereb. Cortex 10 (12) (2000) 1233–1241.
[17] W.A. Johnston, V.J. Dark, In defense of intraperceptual theories of attention, J. Exp. Psychol. Hum. Percept. Perform. 8 (3) (1982) 407–421.
[18] S.M. Kosslyn, G. Ganis, W.L. Thompson, Neural foundations of imagery, Nat. Rev. Neurosci. 2 (9) (2001) 635–642.
[19] J.L. Lancaster, T.G. Glass, B.R. Lankipalli, H. Downs, H.S. Mayberg, P.T. Fox, A modality-independent approach to spatial normalization of tomographic images of the human brain, Hum. Brain Mapp. 3 (1995) 209–223.
[20] S.J. Luck, S.A. Hillyard, Spatial filtering during visual search: evidence from human electrophysiology, J. Exp. Psychol. Hum. Percept. Perform. 20 (5) (1994) 1000–1014.
[21] E.D. Lumer, G.M. Edelman, G. Tononi, Neural dynamics in a model of the thalamocortical system. I. Layers, loops and the emergence of fast synchronous rhythms, Cereb. Cortex 7 (1997) 207–227.
[22] G.R. Mangun, Neural mechanisms of visual selective attention, Psychophysiology 32 (1) (1995) 4–18.
[23] G.R. Mangun, S.A. Hillyard, S.J. Luck, Electrocortical substrates of visual selective attention, in: D. Meyer, S. Kornblum (Eds.), Attention and Performance XIV, MIT Press, Cambridge, MA, 1993, pp. 219–243.
[24] G.R. Mangun, J.B. Hopfinger, A.P. Jha, Integrating electrophysiology and neuroimaging in the study of brain function, Adv. Neurol. 84 (2000) 35–49.
[25] G.R. Mangun, J.B. Hopfinger, C.L. Kussmaul, E.M. Fletcher, H.J. Heinze, Covariations in ERP and PET measures of spatial selective attention in human extrastriate visual cortex, Hum. Brain Mapp. 5 (4) (1997) 273–279.
[26] A. Martinez, L. Anllo-Vento, M.I. Sereno, L.R. Frank, R.B. Buxton, D.J. Dubowitz, E.C. Wong, H. Hinrichs, H.J. Heinze, S.A. Hillyard, Involvement of striate and extrastriate visual cortical areas in spatial attention, Nat. Neurosci. 2 (4) (1999) 364–369.
[27] A. Martinez, F. DiRusso, L. Anllo-Vento, M.I. Sereno, R.B. Buxton, S.A. Hillyard, Putting spatial attention on the map: timing and localization of stimulus selection processes in striate and extrastriate visual areas, Vision Res. 41 (10–11) (2001) 1437–1457.
[28] A. Mehta, I. Ulbert, C.E. Schroeder, Intermodal selective attention

in monkeys. I: Distribution and timing of effects across visual areas, Cereb. Cortex 10 (2000) 343–358.
[29] B.C. Motter, Focal attention produces spatially selective attention in visual cortical areas, V1, V2, and V4 in the presence of competing stimuli, J. Neurophysiol. 70 (1993) 909–919.
[30] T. Noesselt, S.A. Hillyard, M. Woldorff, T. Hagner, L. Jaencke, C. Tempelmann, H. Hinrichs, H.J. Heinze, Delayed striate cortical activation during spatial attention, Neuron, in press.
[31] K.M. O'Craven, B.R. Rosen, K.K. Kwong, A. Treisman, R.L. Savoy, Voluntary attention modulates fMRI activity in human MT-MST, Neuron 18 (4) (1997) 591–598.
[32] C.A. Pelizzari, G.T. Chen, D.R. Spelbring, R.R. Weichselbaum, C.T. Chen, Accurate three-dimensional registration of CT, PET, and/or MR images of the brain, J. Comput. Assist. Tomogr. 13 (1) (1989) 20–26.
[33] F.J. Perrin, O. Pernier, O. Bertrand, J.F. Echallier, Spherical splines for scalp potential and current density mapping, Electroencephalogr. Clin. Neurophys. 72 (1989) 184–187.
[34] M.I. Posner, S. Dehaene, Attentional networks, Trends Neurosci. 17 (2) (1994) 75–79.
[35] M.D. Rugg, P. Walla, A.M. Schloerscheidt, P.C. Fletcher, C.D. Frith, R.J. Dolan, Neural correlates of depth of processing effects on recollection: evidence from brain potentials and positron emission tomography, Exp. Brain Res. 123 (1–2) (1998) 18–23.
[36] M. Scherg, Functional imaging and localization of electromagnetic brain activity, Brain Topogr. 5 (1992) 103–111.
[37] M.I. Sereno, A.M. Dale, J.B. Reppas, K.K. Kwong, J.W. Belliveau, T.J. Brady, B.R. Rosen, R.B.H. Tootell, Borders of multiple visual areas in humans revealed by functional magnetic resonance imaging, Science 258 (1995) 889–893.
[38] G.L. Shulman, M. Corbetta, R.L. Buckner, M.E. Raichle, J.A. Fiez, F.M. Miezin, S.E. Petersen, Top-down modulation of early sensory cortex, Cereb. Cortex 7 (3) (1997) 193–206.
[39] J. Talairach, P. Tournoux, Co-Planar Stereotaxic Atlas of the Human Brain, Thieme, New York, 1988.
[40] G. Tononi, O. Sporns, G.M. Edelman, Reentry and the problem of integrating multiple cortical areas: simulation of dynamic integration in the visual system, Cereb. Cortex 2 (1992) 310–335.
[41] R.B. Tootell, N. Hadjikhani, E.K. Hall, S. Marrett, W. Vanduffel, J.T. Vaughan, A.M. Dale, The retinotopy of visual spatial attention, Neuron 21 (6) (1998) 1409–1422.
[42] L. Ungerleider, J.V. Haxby, 'What' and 'where' in the human brain, Curr. Opin. Neurobiol. 4 (1994) 157–165.
[43] L.G. Ungerleider, M. Mishkin, in: D.J. Ingle, M.A. Goodale, R.J.W. Mansfield (Eds.), Analysis of Visual Behavior, MIT Press, Boston, 1982, pp. 549–586.
[44] M.G. Woldorff, P.T. Fox, M. Matzke, J.L. Lancaster, S. Veeraswamy, F. Zamarripa, M. Seabolt, T. Glass, J.H. Gao, C.C. Martin, P. Jerabek, Retinotopic organization of early visual spatial attention effects as revealed by PET and ERPs, Hum. Brain Mapp. 5 (1997) 280–286.
[45] M.G. Woldorff, M. Matzke, F. Zamarripa, P.T. Fox, Hemodynamic and electrophysiological study of the role of the anterior cingulate in target-related processing and selection for action, Hum. Brain Mapp. 8 (2–3) (1999) 121–127.